UNIVERSITY OF TORONTO

EXPERIMENTS ON DUAL BAND EHF CONTROLLED BEAM ANTENNAS FOR FREQUENCY HOPPED SIGNALS

PHASE-C

by

J. L. Yen

P. Kremer

and

N. Amin

June 20, 1988

For Department of Communications

under

DSS Contract 36100-6-3562/01-ST

EXPERIMENTS ON DUAL BAND EHF CONTROLLED BEAM ANTENNAS FOR FREQUENCY HOPPED SIGNALS

PHASE-C

1. INTRODUCTION:

In the phase-B Study of this Contract[1,2] the concept of dual-band nulling for anti-jamming in EHF SATCOM using frequency hopped signals was validated by preliminary experiments. This experimental investigation is continued in the present Phase-C study where detailed nulling performance under various scenarios is studied. Particular attention is directed towards the comparison of dual-band and narrow-band nulling performance in a static environment. The results with 60 db dynamic range show that in static performance, dual-band nulling has no apparent advantage over narrow-band nulling alone. However, since the weighting coefficients used in the system do not have sign control, phase adjustment over 360 degree range requires setting the length of one of the two transmission lines connecting the antenna elements, thus an improper length could degrade the performance of dual-band nulling more severely. The result is not unexpected because the main aim of dual-band nulling is to have fast acting nulling under a frequency hopping environment. Since an adaptive algorithm has not been selected, an adaptive dual-band controller was not implemented for this investigation.

A parallel analytical investigation is the Maximum Signal to Jammer & Noise criterion for nulling. In Phase-B study, the criterion was successfully applied to a phased array with known directions of desired signals using the conjugate gradient algorithm. However, because of the computational burden the algorithm is not easy to implement. A new algorithm using an estimate of the conjugate gradient is introduced. This algorithm requires approximately twice the computing complexity of the simple LMS algorithm, and is found to work almost as well as conjugate gradient.

2. DUAL-BAND AND NARROW-BAND NULLING, A STATIC PERFORMANCE COMPARISON:

The dual-band beam control for protection of EHF SATCOM using frequency hopped signals proposed in this series of Contracts is to combine a slow acting broad-band nulling with a fast-acting narrow-band nulling for superior antijamming performance. An experimental test bench with a two element receiving array together with a single desired signal transmitter as well as a single jammer was established. So far only CW signal and jammer have been implemented. Using the test bench various aspects of nulling performance using commercial grade components were experimentally investigated. In the Phase-C study reported here, the experiment on dual-band nulling carried out in Phase-B study is continued.

2.1 The Experimental Setup:

The experimental setup is mainly the same as before and is shown in Fig.1. The broad-band IF is at 500-1000 Mhz with two adjustable complex weights with labels (1,2) and (3,4). The two complex signals are further down converted to the narrow-band 40 Mhz second IF, with a bandwidth of 4 Mhz, using a common voltage controlled second local oscillator. Two adjustable narrow-band complex weights with the same labels are used to implement narrow-band nulling. The received desired and jamming signals are measured using a tracking spectral analyzer in time division multiplex by switching the signal source between the signal and jammer transmitting antennas. The system has a dynamic range of 60 db. In the early stage of the investigations interference of some very strong local UHF transmitters were detected. When tracking through the IF spectrum the receiver locks on to the interfering signal and loses track of the stepping transmitter. Or, when nulling, the system attempts to null these signals and produces wrong weights.The second IF is therefore modified to minimize these interfering signals. However, it was noted in some of the runs certain jammer power peaks were not reproducible, thus there may still be some external interferences not completely removed.

2.2 The Experimental Procedure:

The experimental procedure mainly parallels the work of Phase-B, hence the details will not be repeated here. All experiments have been conducted under the following conditions:

The offset in the focal plane and the position on the cluster axis remain constant.

The separation of the two transmitting horns is fixed at 30mm.

Both horns transmit with equal power.

The nulling must not reduce the desired signal by more than 3 db.

To establish the desired signal level before nulling the following steps are executed: If broad-band nulling is to be performed the attenuators of the first IF are used to adjust the phases of both receiver channels for maximum signal. With this setting the band is scanned and the received signal for all frequency steps are recorded and stored as a reference. This pre-null reference is used to normalize the the measured powers after nulling. For narrow-band nulling the same procedure is applied for the setting of the second IF components. The broad-band weights are set to unity.

Nulling can be performed at steps of .75, 2.5, 5, 10, 25, 50 and 100 Mhz.

2.3 Frequency dependence of narrow-band nulling weights:

The frequency dependence of narrow-band nulling weights are shown in Figs. 2-5. The across-band nulling is performed with 2.5 Mhz steps resulting in 184 sets of 4 weights. The weights are given in db channel attenuation. Observe that weights 1 and 2, which are for antenna element 1, have about 10 db less attenuation than the weights 3 and 4 for antenna element 2. This is the result of the relative positions of the two antenna beams with respect to the signal and jammer transmitter positions. It is not clear what caused the large dip for weight 1 at 900 Mhz and the variation of weight 4 below 650 Mhz. When a weight has large attenuation, very little signal is coming through for nulling, hence the above may be due to phase variation required to null the jammer within the band.

2.4 Dual-Band Nulling:

Figs. 6-9 show the results of dual-band nulling under various conditions. Broad-band nulling is first performed at the frequency indicated. Narrow-band nulling is then performed at 50 Mhz steps and the weights are stored. In the following scan

these weights were applied at the appropriate frequencies as the frequency increases in the scan, and the desired signal power and the jammer power are measured in turn and plotted. The trace with the heavy line represents the jammer after nulling with the weights applied. The desired signal after nulling is shown in the lighter trace and it differs from the pre-null reference by less than -3 db. It is expected that what ever are the broad band weights required for broad-band nulling, further narrow-band nulling at a frequency should reduce the jammer to signal ratio. It is seen that indeed in most situations the jammer power at the narrow-band nulling frequency is below the 60 db dynamic range of the system to be properly measured. However, Figs. 8 & 9 show that with broad-band nulling performed at 800 & 900 Mhz, further narrow-band nulling around 650-750 Mhz do not produce deep jammer nulls at the narrow-band nulling frequency. In fact the variation of the jammer level in this frequency range have the same appearance in the two Figures. A possible cause for this strange behaviour is that the broad-band weights may have reduced one or two of the four real signal components to very low levels so that they are no longer available for narrow-band nulling to function. More detailed experiments are required to clarify this phenomenon.

2.5 Narrow-Band Nulling:

Figs. 10-12 show results of narrow-band nulling alone in 50, 10 and 2.5 Mhz steps. In these experiments the broad-band weights are set to unity. The resulting signal and jammer powers are plotted. In addition, the pre-null signal is also shown in the 2.5 Mhz step data to show that the desired signal is degraded by less than 3 db due to nulling. In general the static performance of narrow-band nulling alone is better than that of dual-band nulling. The data of 10 Mhz steps show particularly low jammer to signal ratio because for that experiment the length of one of the transmission lines was very carefully adjusted.

2.6 Further Work on Dual-band Nulling:

To determine more accurately the performance of dual-band and narrow-band nulling, the system need be modified as follows:

The second IF bandwidth need be lowered to say 200 Khz so as to reduce the effect of external interference.

Weighting coefficient sign control be introduced to have assurance of 360 degree phase adjustment.

The useful dynamic range of the system must be increased by at least 10 db.The conclusion from these experiments is that in a static environment dual-band nulling does not appear to perform as well as narrow-band nulling alone. This is probably due to the previously mentioned reduction of some signal components by the broad-band weights. However, since the main advantage of dual-band nulling is seen in the combination of a slow acting broad-band nuller and a fast acting narrow-band nuller, it is necessary to measure the convergence time in a dynamic frequency hopping environment using an appropriate nulling algorithm before the advantage of dual-band nulling can be properly evaluated.

3. A MODIFIED CONJUGATE GRADIENT ALGORITHM:

In previous studies of this Contract a Maximum Signal to Jammer and Noise Ratio criterion for antijamming using a phased array was proposed and that the conjugate gradient method was shown to be able to obtain the weights for very low jammer to signal ratio using a small number of iterations. However, the conjugate gradient method requires the calculation of the Hessian matrix at every step resulting in high computational burden. To arrive at a practical algorithm for optimisation under the maximum signal to jammer and noise ratio criterion a modified form of the conjugate gradient method is introduced. The computational burden using the approach is about twice that of the very fast and simple LMS algorithm. The resulting signal to jammer ratio after nulling is slightly inferior to that obtainable using the full conjugate gradient method, but is fully acceptable in most applications. In the following the algorithm is described and simulation results for a linear phased array are presented. It is found that the algorithm is both fast and yielding high jammer protection.

3.1. The Criterion:

In two previous Reports[1,2], a new criterion for beam control was introduced. Fig.13 shows a block diagram of the system. The criterion is to maximize the ratio of signal power and jammer plus noise power SJNR

$$\max \quad \mathbf{W}^h \mathbf{R}_{xx} \mathbf{W} / \mathbf{W}^h \mathbf{R}_{zz} \mathbf{W} \qquad (1)$$

where $\mathbf{R}_{xx}$ and $\mathbf{R}_{zz}$ are the correlation matrices of the signal and jammer plus noise respectively. W is the element weighting vector, and ^{h} denotes conjugate transpose. In a phased array, as investigated previously, the jammer plus noise signal vector Z(t) can be obtained from the received signal vector X(t) by using a blocking matrix **B** to remove the desired signals from the known directions

$$\mathbf{Z}(t) = \mathbf{B}\,\mathbf{X}(t) \tag{2}$$

For a single user in direction u from broadside, a possible blocking matrix is

$$\mathbf{B} = \begin{bmatrix} 1 & -\text{expjkd}_1\text{sinu} & 0 & \text{------} \\ 0 & 1 & -\text{expjk}(d_2\text{-}d_1)\text{sinu} & \text{------} \\ \text{------} & & & \text{------} \\ & \text{------} & 1 & -\text{expjk}(d_L\text{-}d_{L\text{-}1})\text{sinu} \end{bmatrix} \tag{3}$$

where the L elements are located at d1 to dL. The optimal weight vector Wopt is the eigen vector of the generalized eigen value problem

$$\mathbf{R}_{xx}\mathbf{W}_{opt} = \lambda_{max}\mathbf{R}_{zz}\mathbf{W}_{opt} \tag{4}$$

The two correlation matrices have complex coefficients representing phase differences to the different array elements. As discussed previously, the criterion tends to protect the desired users while nulling out the jammers.

3.2. The Algorithm:

In the last Report, the Fletcher-Reeves conjugate gradient method was successfully used to find the optimum weights as defined by the generalized eigen value problem. The search direction $\mathbf{P}_i$ in step i is conjugate to that of the jth step with respect to **H**, the Hessian matrix of the problem according to

$$\mathbf{P}_i^h\,\mathbf{H}\,\mathbf{P}_j = 0, \quad i=j \tag{5}$$

An optimum step size along the search direction is then used to complete one iteration. Since the step size can be large for an appropriate direction, fast convergence is achieved.

However, the method requires the estimates of both the gradient vector and the Hessian matrix at every iteration, a very computing intensive operation. In the following a modified conjugate gradient approach[3] is presented which greatly reduces the computational requirements without appreciably degrading the achievable signal to jammer ratio.

The receiver first estimates the covariance matrices of n block of length T snapshots as

$$\mathbf{R}_{xx}^{n} = (1/T) \sum_{t=(n-1)T+1}^{nT} \mathbf{X}(t)\mathbf{X}(t)^{h}$$

$$\mathbf{R}_{zz}^{n} = (1/T) \sum_{t=(n-1)T+1}^{nT} \mathbf{Z}(t)\mathbf{Z}(t)^{h} \qquad (6)$$

For the objective function of (4) using the above covariance matrices, the estimated gradient vector is

$$\mathbf{G}_n = [\mathbf{R}_{xx}^{n} - \lambda_n \mathbf{R}_{zz}^{n}] \mathbf{W}_{n-1} \qquad (7)$$

where the scale factor $1 / (\mathbf{W}_{n-1}^{h} \mathbf{R}_{zz}^{n} \mathbf{W}_{n-1})$ is omitted to eliminate its effect on iteration number. The search direction is obtained by approximating the vector $\mathbf{P}^{t}\mathbf{H}$ with

$$\gamma_{n-1} = \mathbf{G}_n - \mathbf{G}_{n-1} \qquad (8)$$

The search vector $\mathbf{P}_n$ satisfies

$$\gamma_{n-1}^{h} \mathbf{P}_n = 0 \qquad (9)$$

and for $\lambda_n - \lambda_{n-1}$

$$(\mathbf{W}_n - \mathbf{W}_{n-1})^{h} [\mathbf{R}_{xx}^{n} - \lambda_n \mathbf{R}_{zz}^{n}] \mathbf{P}_n = 0 \qquad (10)$$

or

$$\mathbf{P}_{n-1}^{h}\,[\mathbf{R}_{xx}^{n} - \lambda_n \mathbf{R}_{zz}^{n}]\,\mathbf{P}_n = 0 \qquad (11)$$

This condition is also satisfied for $\mathbf{P}_{n-1}$, $\mathbf{P}_n$ being the generalized eigenvectors of (4). $\mathbf{P}_n$ becomes

$$\mathbf{P}_n = \mathbf{G}_n - (\gamma_{n-1}^{h}\,\mathbf{G}_n / \gamma_{n-1}^{h}\,\mathbf{P}_{n-1})\,\mathbf{P}_{n-1} \qquad (12)$$

To update the weights, the step size un is

$$\frac{\max\,(\mathbf{W}_n + \mu_n\mathbf{P}_n)^{h}\,\mathbf{R}_{xx}^{n}\,(\mathbf{W}_n + \mu_n\mathbf{P}_n)}{\mu_n\;\;(\mathbf{W}_n + \mu_n\mathbf{P}_n)^{h}\,\mathbf{R}_{zz}^{n}\,(\mathbf{W}_n + \mu_n\mathbf{P}_n)} \qquad (13)$$

The step size υ_n required to update $\mathbf{W}_n$ is chosen such that SJNR is maximized in the direction of $\mathbf{P}_n$. Using the following parameters

$$\begin{aligned}
A &= 2\,\mathrm{Re}(\mathbf{P}_n^{h}\,\mathbf{R}_{xx}^{n}\,\mathbf{W}_{n-1})\,(\mathbf{W}_{n-1}^{h}\,\mathbf{R}_{zz}^{n}\,\mathbf{W}_{n-1}) \\
&\quad - 2\,\mathrm{Re}(\mathbf{P}_n^{h}\,\mathbf{R}_{zz}^{n}\,\mathbf{W}_{n-1})\,(\mathbf{W}_{n-1}^{h}\,\mathbf{R}_{xx}^{n}\,\mathbf{W}_{n-1}) \\
B &= 2\,(\mathbf{P}_n^{h}\,\mathbf{R}_{xx}^{n}\,\mathbf{P}_n)\,(\mathbf{W}_{n-1}^{h}\,\mathbf{R}_{zz}^{n}\,\mathbf{W}_{n-1}) \\
&\quad - 2\,(\mathbf{P}_n^{h}\,\mathbf{R}_{zz}^{n}\,\mathbf{P}_n)\,(\mathbf{W}_{n-1}^{h}\,\mathbf{R}_{xx}^{n}\,\mathbf{W}_{n-1}) \\
C &= 2\,\mathrm{Re}(\mathbf{P}_n^{h}\,\mathbf{R}_{zz}^{n}\,\mathbf{W}_{n-1})\,(\mathbf{P}_n^{h}\,\mathbf{R}_{xx}^{n}\,\mathbf{P}_n) \\
&\quad - 2\,\mathrm{Re}(\mathbf{P}_n^{h}\,\mathbf{R}_{xx}^{n}\,\mathbf{W}_{n-1})\,(\mathbf{P}_n^{h}\,\mathbf{R}_{zz}^{n}\,\mathbf{P}_n)
\end{aligned} \qquad (14)$$

we have

$$\mu_n = -B - (B^2 - AC)^{1/2} / C \qquad (15)$$

and the update weighting vector W_n is

$$W_n = W_{n-1} + \mu_n \qquad (16)$$

The objective function (4) is W-scale invariant. However, because of the noisy received signal, the magnitudes of the weights may increase and thereby the amplitude of the array output. The signal distortion is avoided if the weight vector norm is held constant

$$W_n^h W_n = \text{constant} \qquad (17)$$

The process is repeated after every new block of signal is received.

Comparing the above algorithm with the familiar LMS algorithm, it is seen that the computational burden is only approximately two times more complex. It is much more simpler than the full conjugate gradient method employed in the previous study[2].

3.3. Simulation Results:

The performance of the adaptive array using **B** in (3) is examined. A 12 element uniform linear array of half wave length spacing is considered. As the number of snapshots per block increases, the array pattern improves. However, this compromises the rate of the array response in a dynamic jamming environment. A block of 32 snapshots is used in all following simulations. The signal is a sine wave with a period of 10 snapshots.

In the first example, one that was investigated using the conjugate gradient method in Phase-B studies,a single desired signal arriving from the array broadside in the presence of a single jammer at 6^o is analyzed. The jammer is inside the 10^o main beam of the quiescent pattern. Independent white noise of normal distribution is added to the simulated desired signal and jamming signal of 40db and 70db above

the noise variance respectively at each element. Since there are many eigen vectors to the maximization problem a well chosen initial vector is needed in order that the adapted weights converge to the correct one. The chosen initial vector is the optimum weighting vector in the presence of no jamming with only the signal and noise present derived analytically from the known direction of the desired signal and system noise. This is the quiescent array and has tapered weights so that the sidelobes are lower than those of a uniformly illuminated array. The adapted pattern after 100 iterations is shown in Fig.14. A deep null of -95 db is steered towards the jammer direction while the pattern still maintains a well distinguished main lobe, its peak is pushed away from the jammer by 3^{o}, and tapered sidelobes. The array weights are independent of the desired signal power and the constant norm constraint of (17) is mainly to prevent output signal amplitude fluctuations. The value of the objective function in (4), namely, the ratio between the output signal power and noise branch power, is plotted against the iteration number in Fig.15. It takes only 7 iterations for the objective function to reach its steady state value and thus only a small number of samples are required for the algorithm to converge. The same example is also analyzed using the full Hessian matrix as described in Phase-B study. The resulting pattern and the convergence are shown in Figs.16-17. The null is deeper and the side lobes are smaller. However it takes 22 iterations for the process to converge and, due to the complexity of computing the Hessian matrix, consuming considerably more computing time.

Finally, the adaptive pattern of the array in the presence of two desired signals, at -20^{o} and $+10^{o}$ of SNR 10 db and 0 db respectively ,in the presence of a single jammer of JNR = 50 db at 0^{o} is shown in Fig.18. The pattern has a null in the jammer direction and two separate main lobes in the desired signal directions with 4 db difference in level due to the signal power difference. The algorithm takes 8 iterations to converge.

3.4. Proposed Further Work On the Modified Conjugate Gradient Algorithm:

Because of its fast convergence and the relatively simplicity, the modified conjugate gradient algorithm shows great promise in real implementation of EHF controlled beam antennas. Simulation of the algorithm applying to two dimensional multi-beam arrays need be first carried out. An experimental real time implementation on a 3-beam array should then be assembled for performance evaluation.

4. REFERENCE

1. J.L.Yen, P.Kremer & N.Amin, "Experiments on Dual Band EHF Controlled-Beam Antennas for Frequency-Hopped Signals", Final Report, DSS File # OST85-00209, July 1986.

2. J.L.Yen, P.Kremer & N.Amin, "Experiments on Dual Band EHF Controlled-Beam Antennas for Frequency-Hopped Signals: Phase B", Final Report, DSS Contract No. 36001-6-3562/01-ST, July 1987.

3. M.S.Bazaraa & C.M.Shetty, "Nonlinear Programming: Theory and Algorithms", Wiley, New York, 1979.

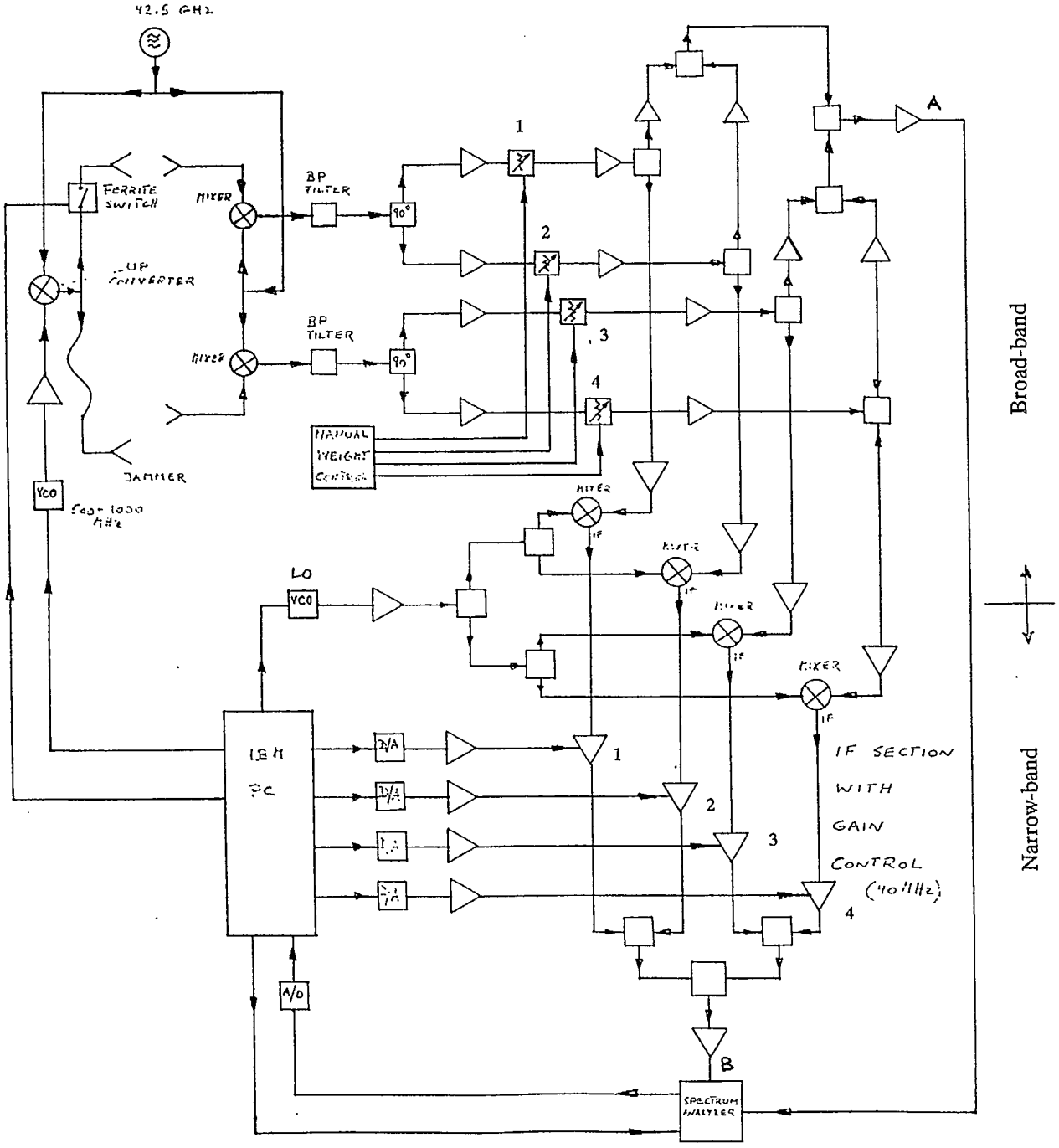

Fig.1 Block Diagram of Dual-Band Nulling System.

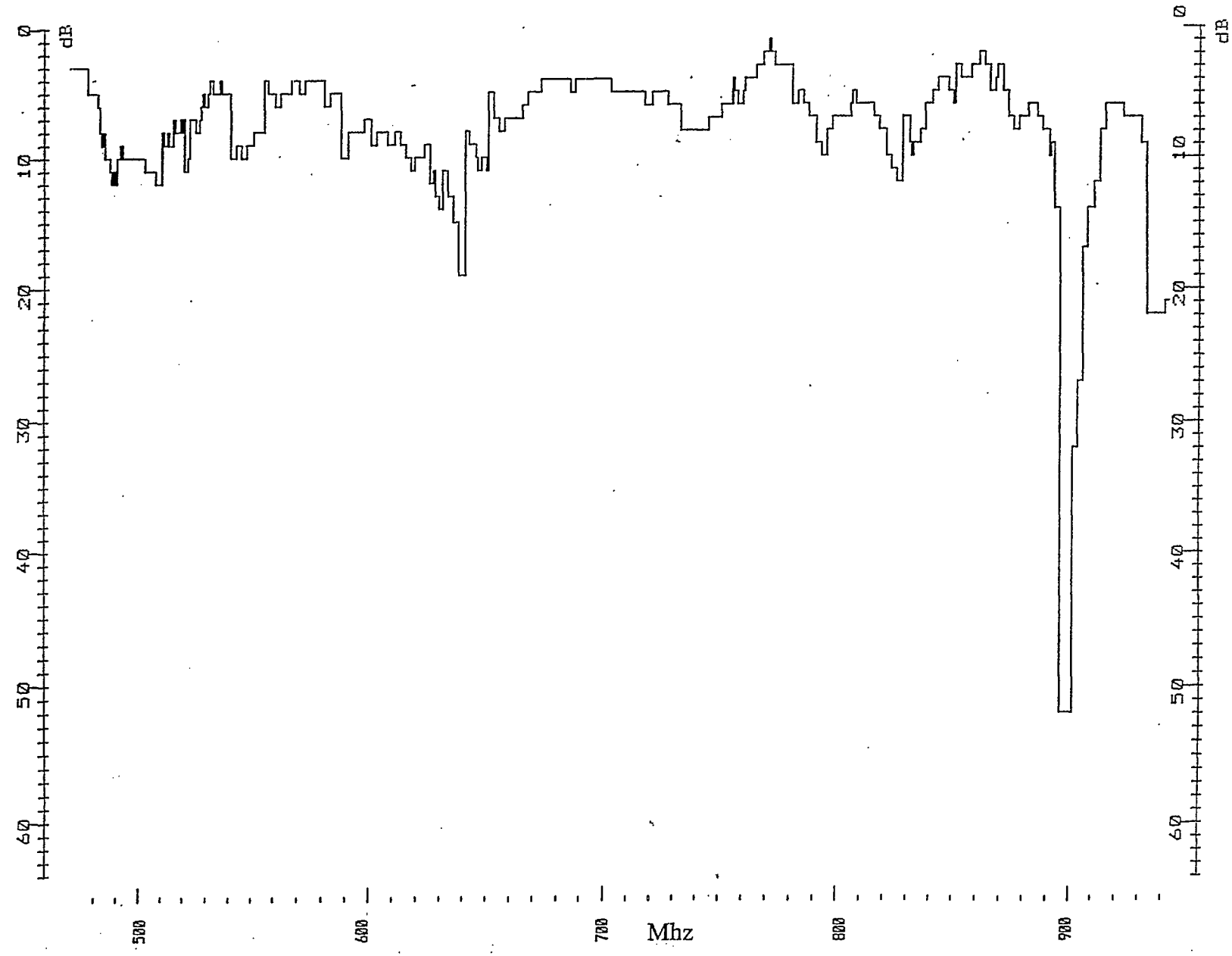

Fig.2 Weight 1 in db attenuation after narrow-band nulling at 2.5 Mhz steps versus broad-band IF frequency in Mhz.

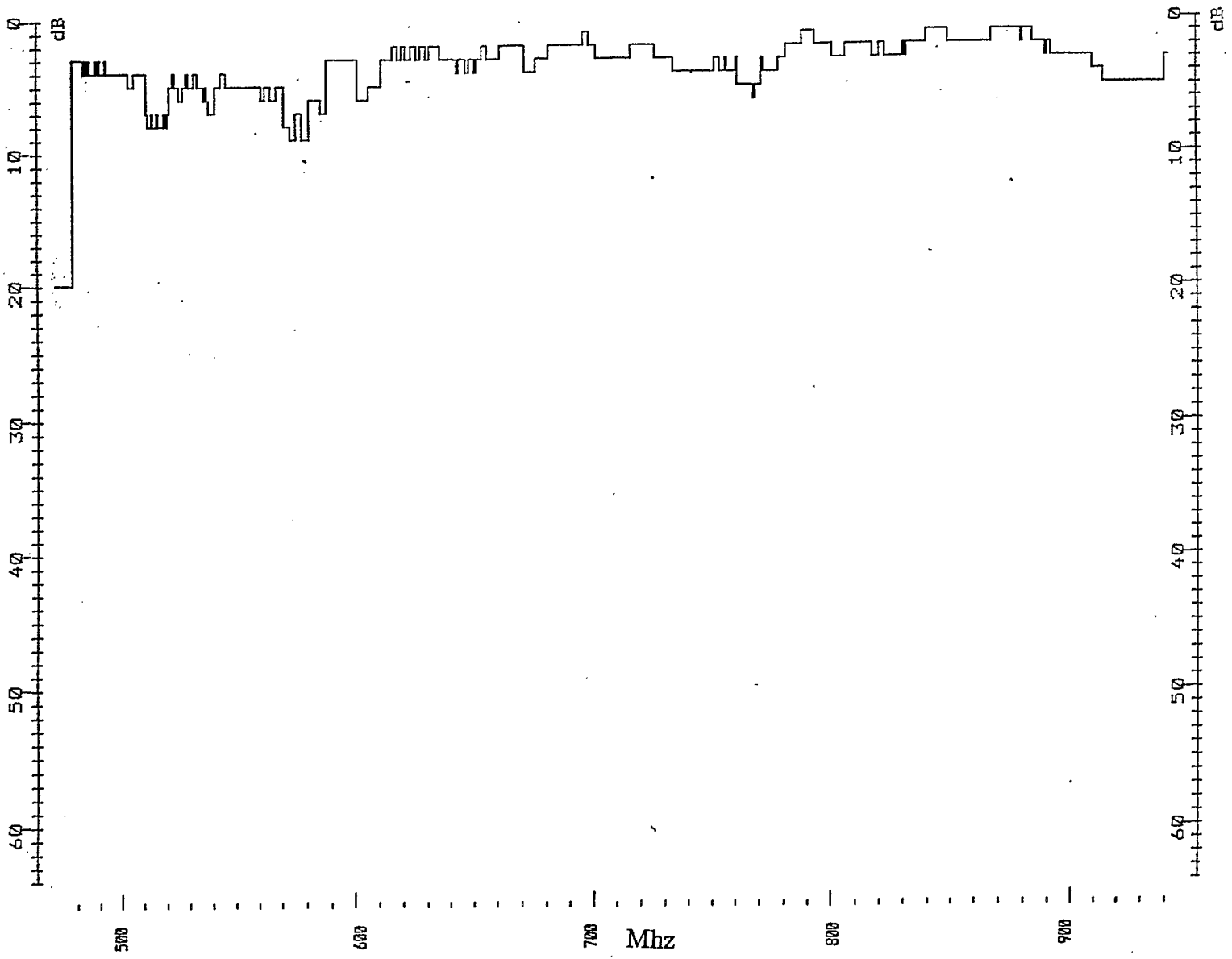

Fig.3 Weight 2 in db attenuation after narrow-band nulling at 2.5 Mhz steps versus broad-band IF frequency in Mhz.

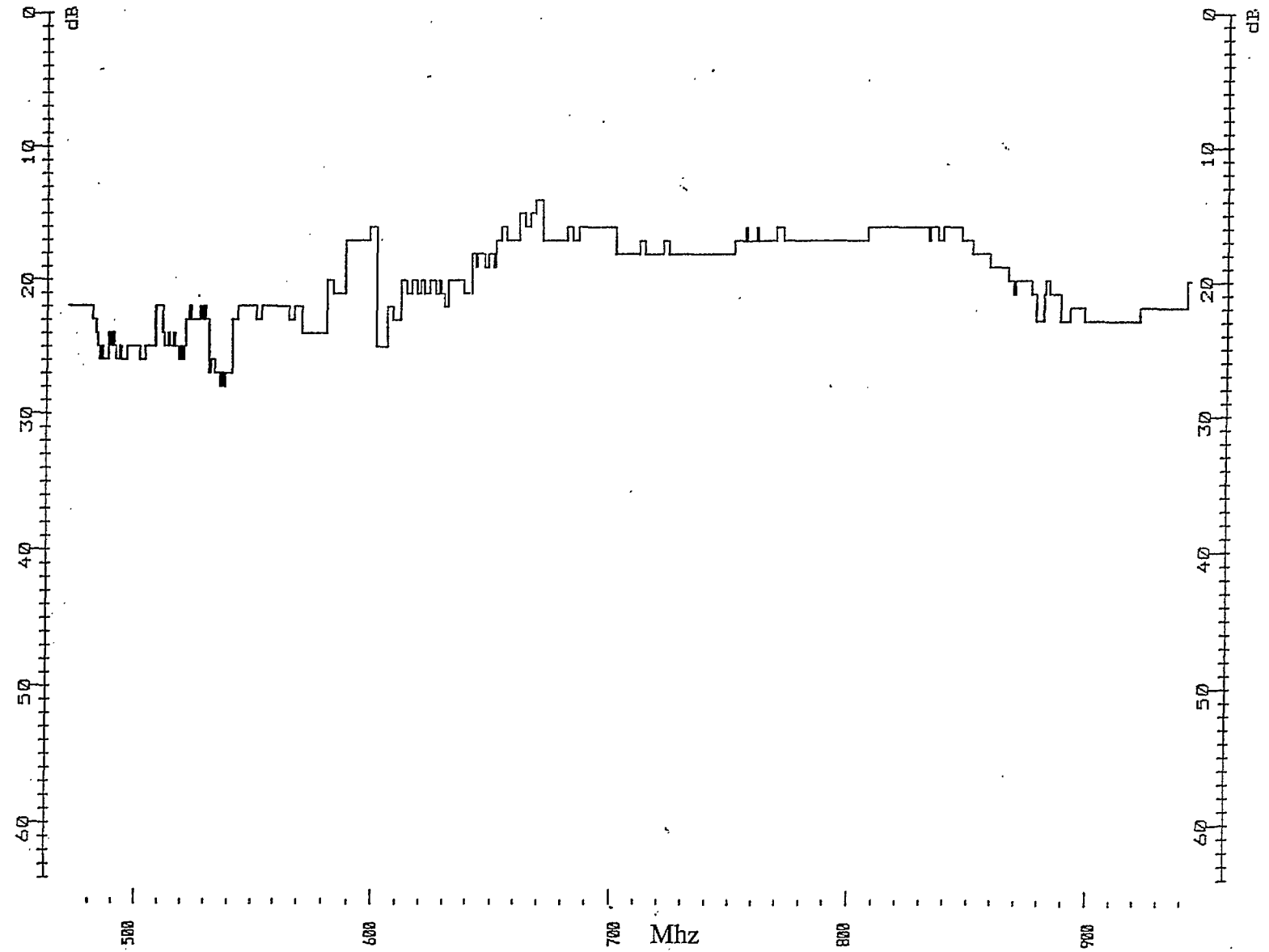

Fig.4 Weight 3 in db attenuation after narrow-band nulling at 2.5 Mhz steps versus broad-band IF frequency in Mhz.

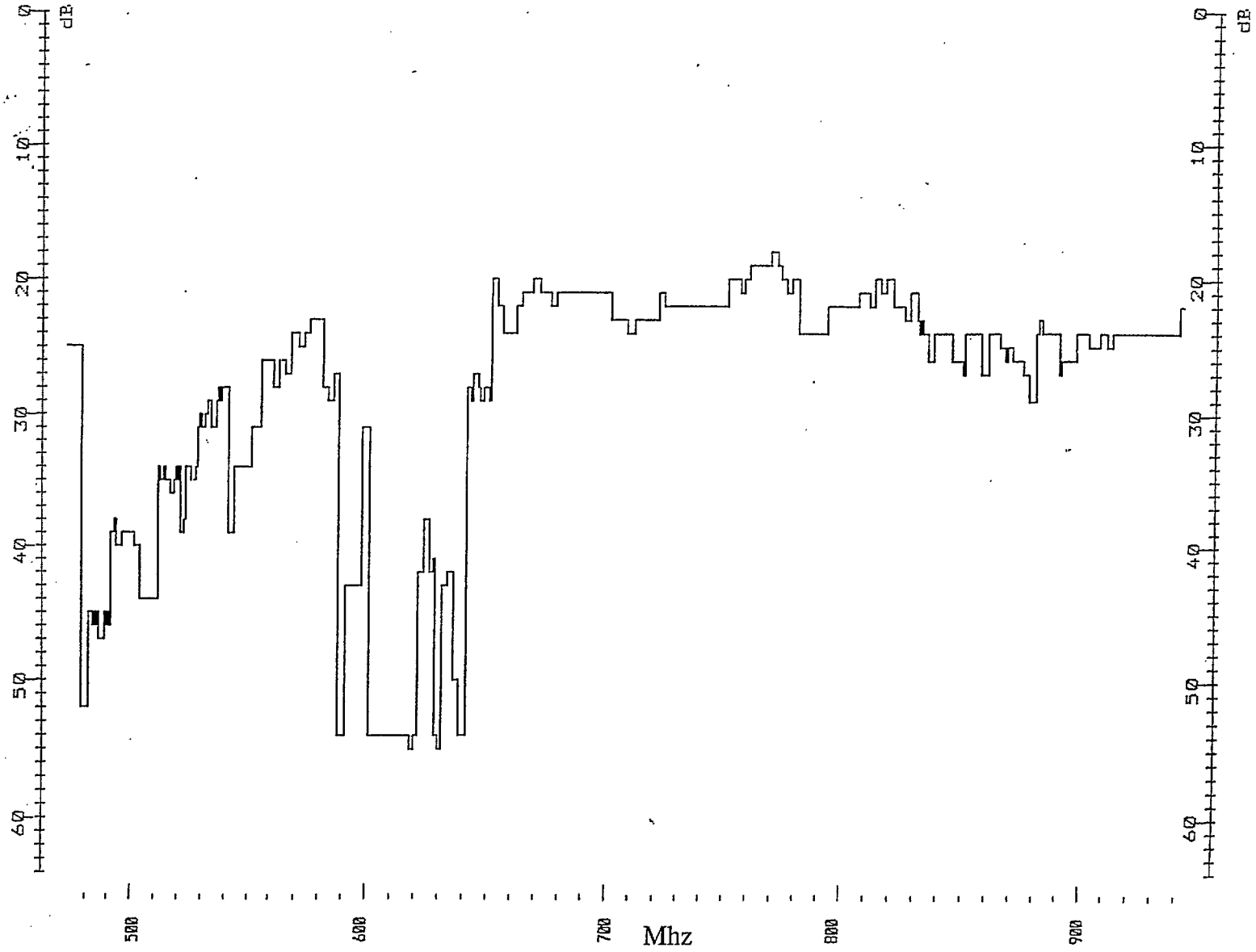

Fig.5 Weight 4 in db attenuation after narrow-band nulling at 2.5 Mhz steps versus broad-band IF frequency in Mhz.

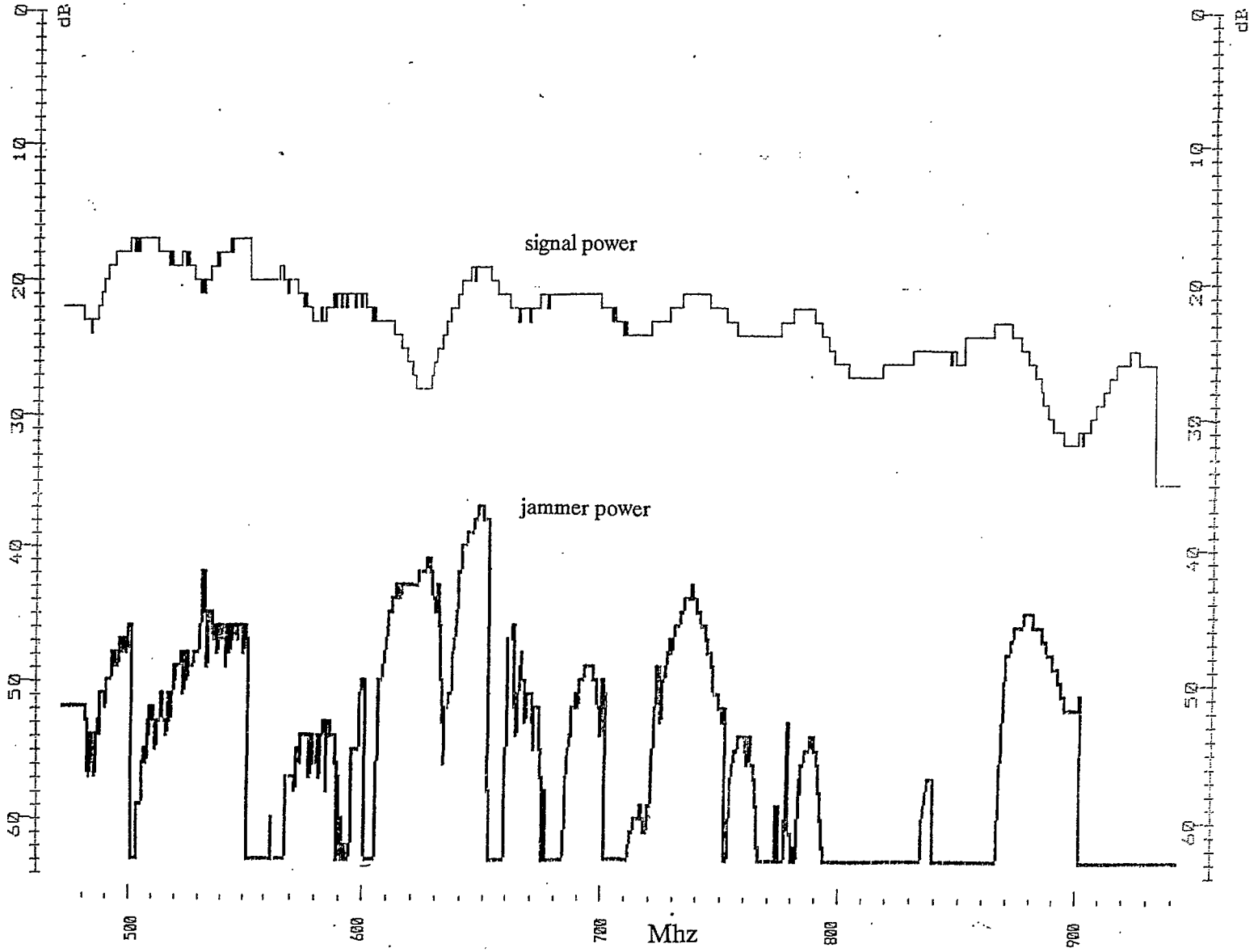

Fig.6 Signal and jammer power in db below arbitrary reference after dual-band nulling. Narrow-band nulling at 50 Mhz steps, broad-band nulling at 600 Mhz.

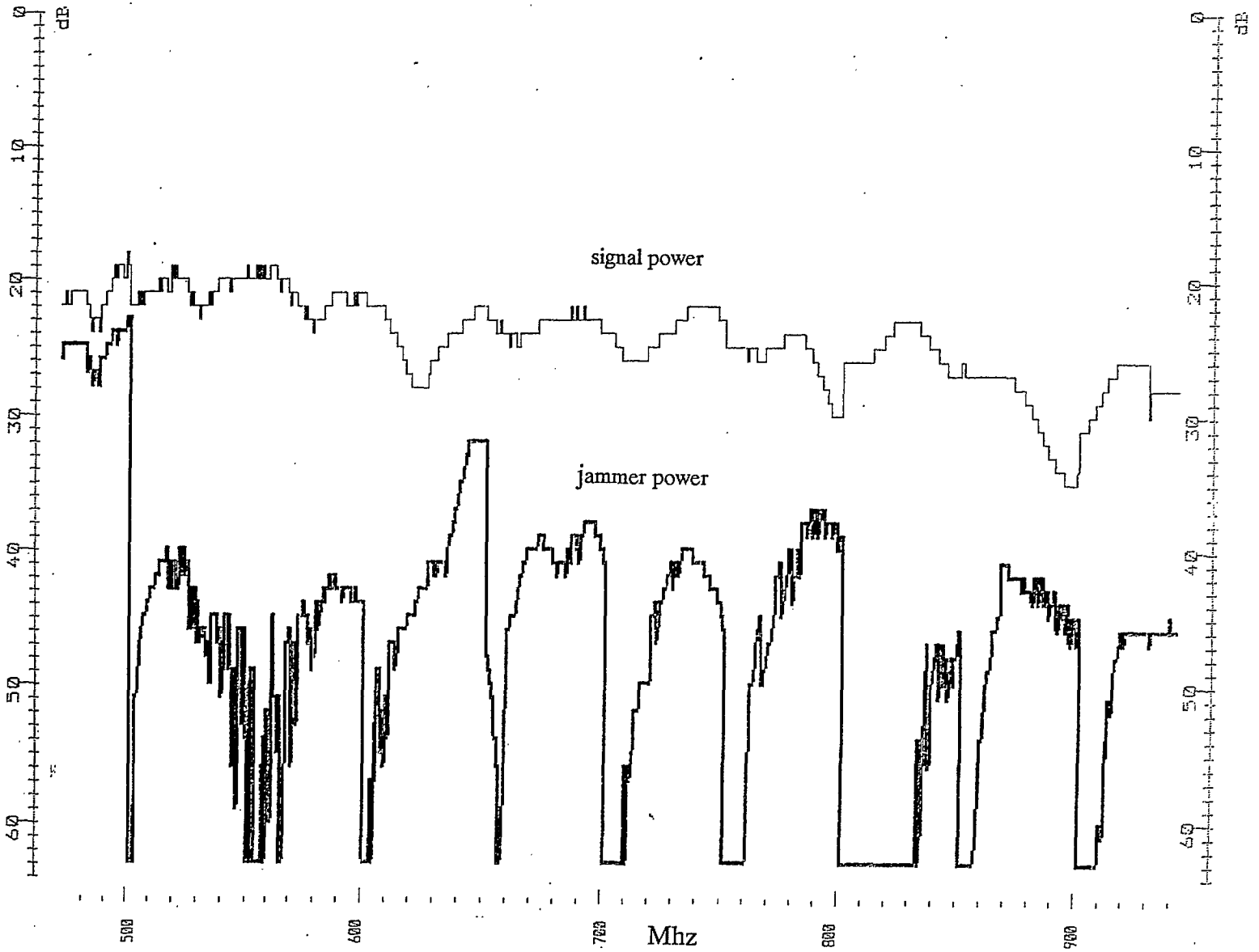

Fig.7 Signal and jammer power in db below arbitrary reference after dual-band nulling. Narrow-band nulling at 50 Mhz steps, broad-band nulling at 700 Mhz.

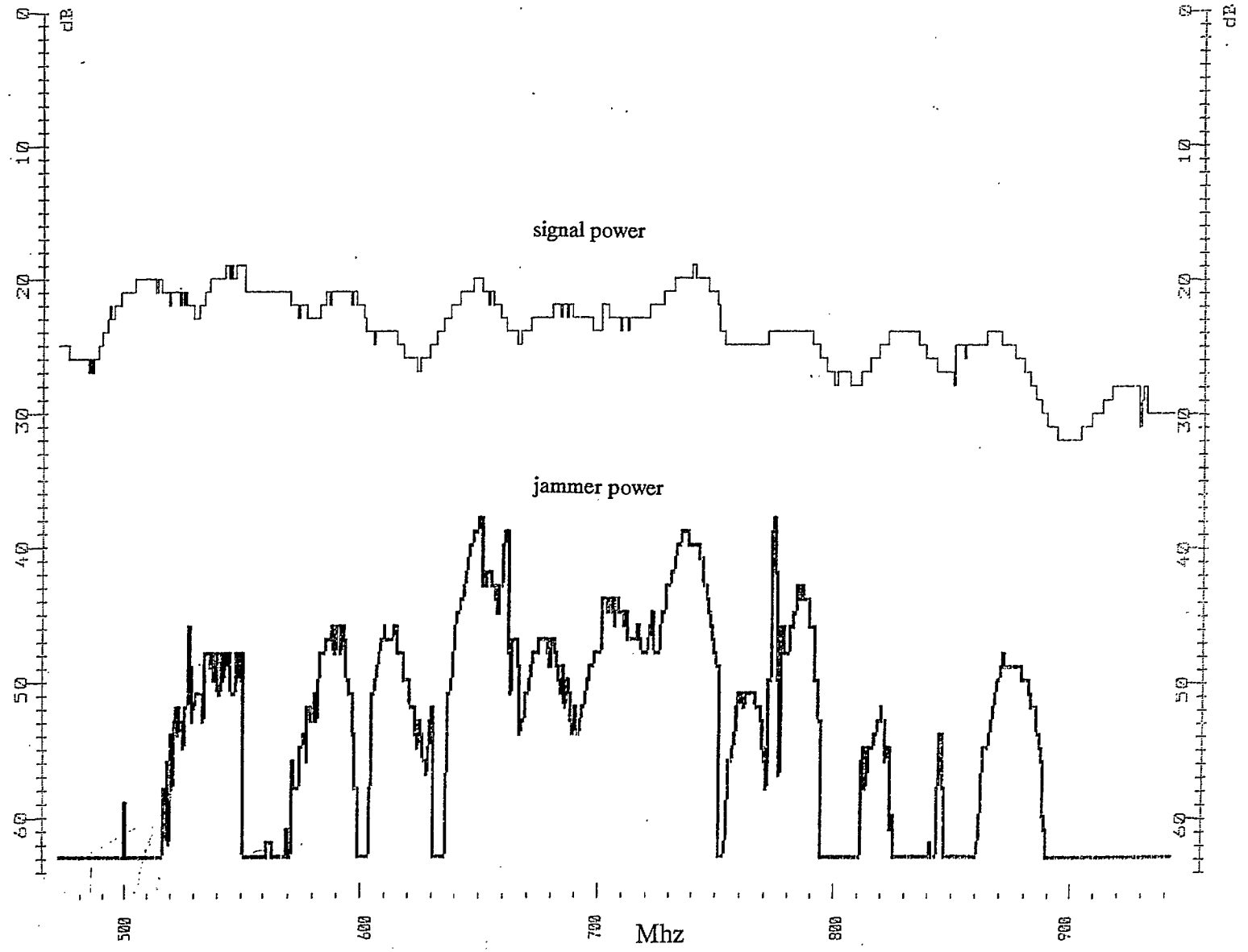

Fig.8 Signal and jammer power in db below arbitrary reference after dual-band nulling. Narrow-band nulling at 50 Mhz steps, broad-band nulling at 800 Mhz.

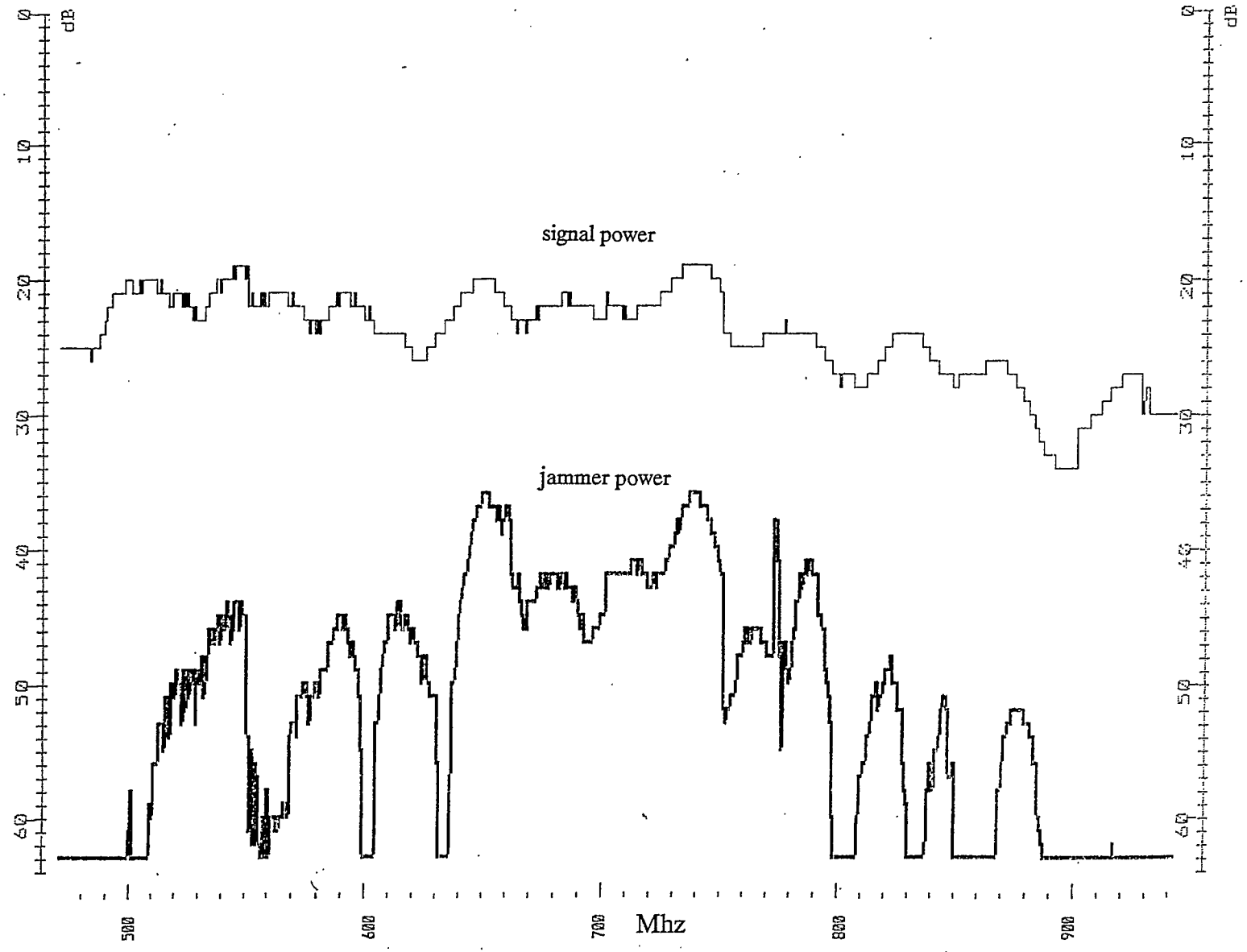

Fig.9 Signal and jammer power in db below arbitrary reference after dual-band nulling. Narrow-band nulling at 50 Mhz steps, broad-band nulling at 900 Mhz.

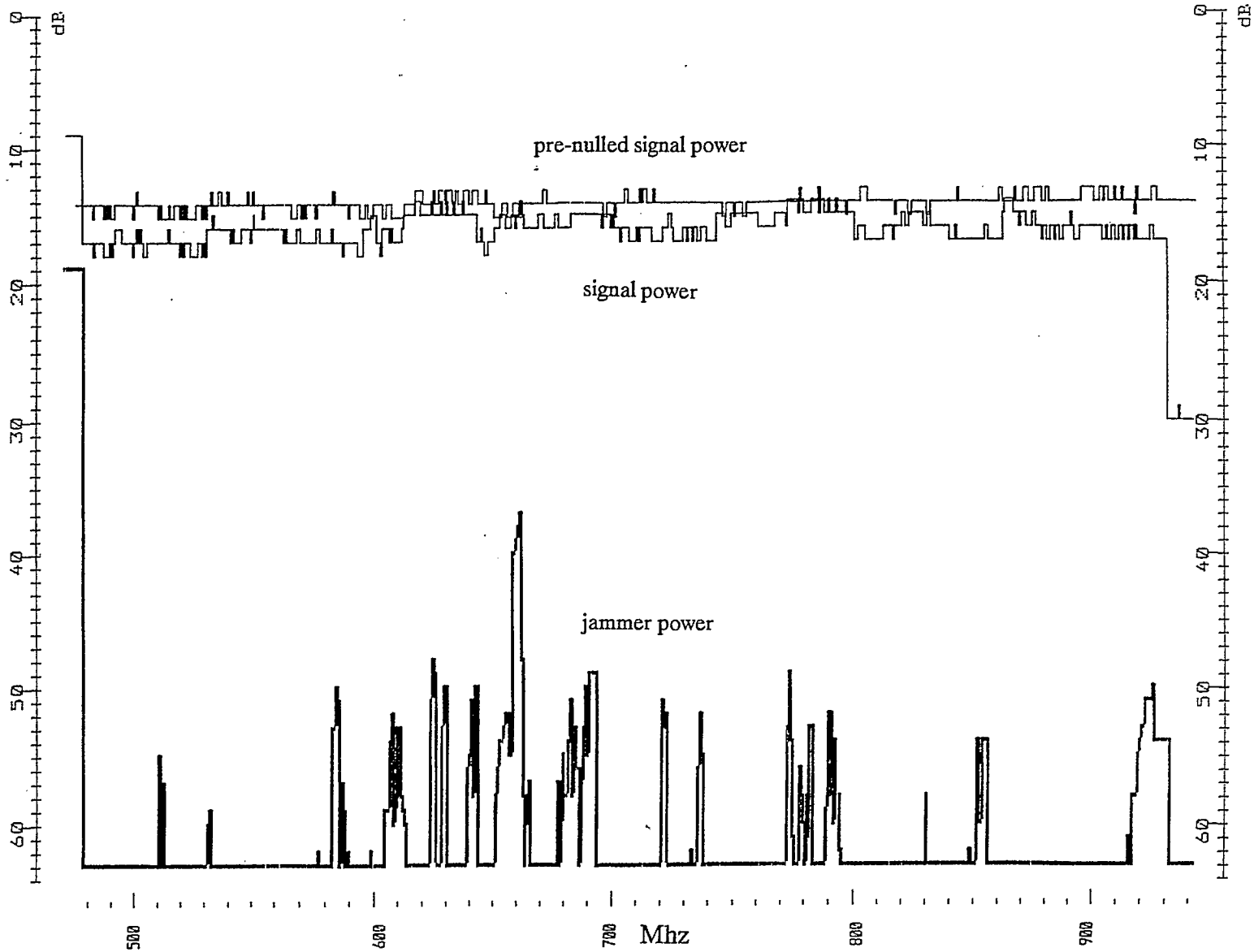

Fig.10 Signal and jammer power and pre-null signal power in db below arbitrary reference after narrow-band nulling at 2.5 Mhz steps. Broad-band weights set to unity.

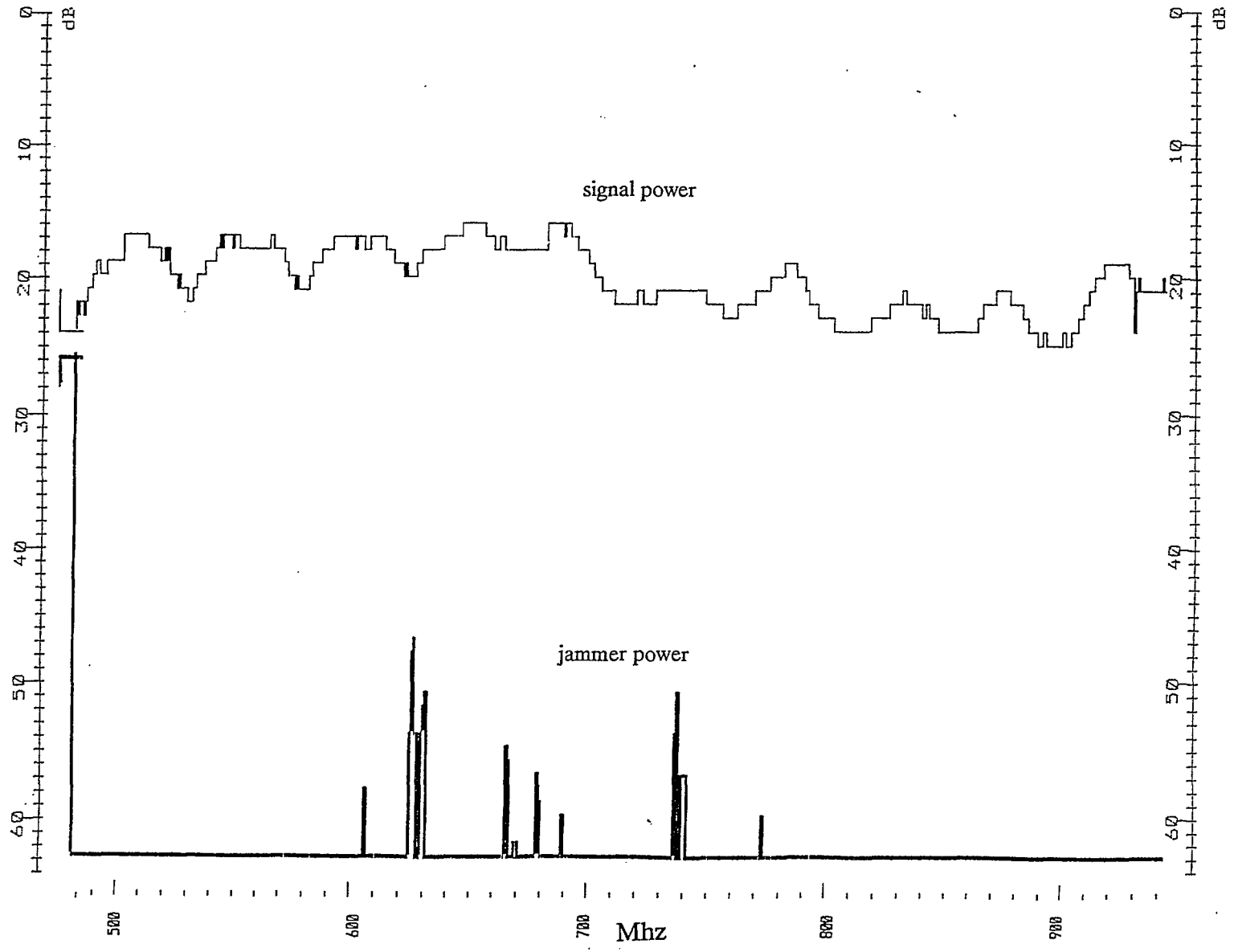

Fig.11 Signal and jammer power in db below arbitrary reference after narrow-band nulling at 10 Mhz steps. Broad-band weights set to unity.

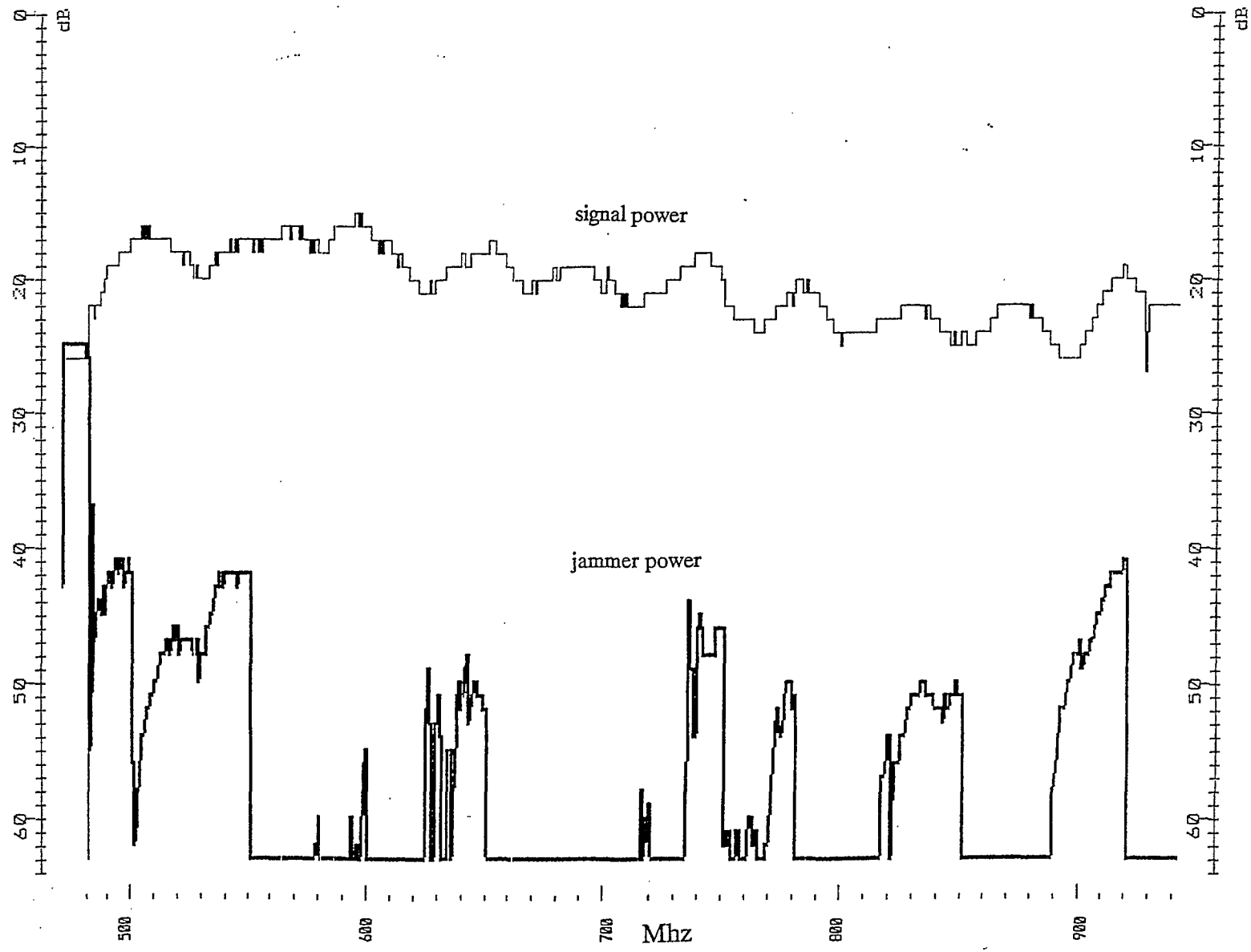

Fig.12 Signal and jammer power in db below arbitrary reference after narrow-band nulling at 50 Mhz steps. Broad-band weights set to unity.

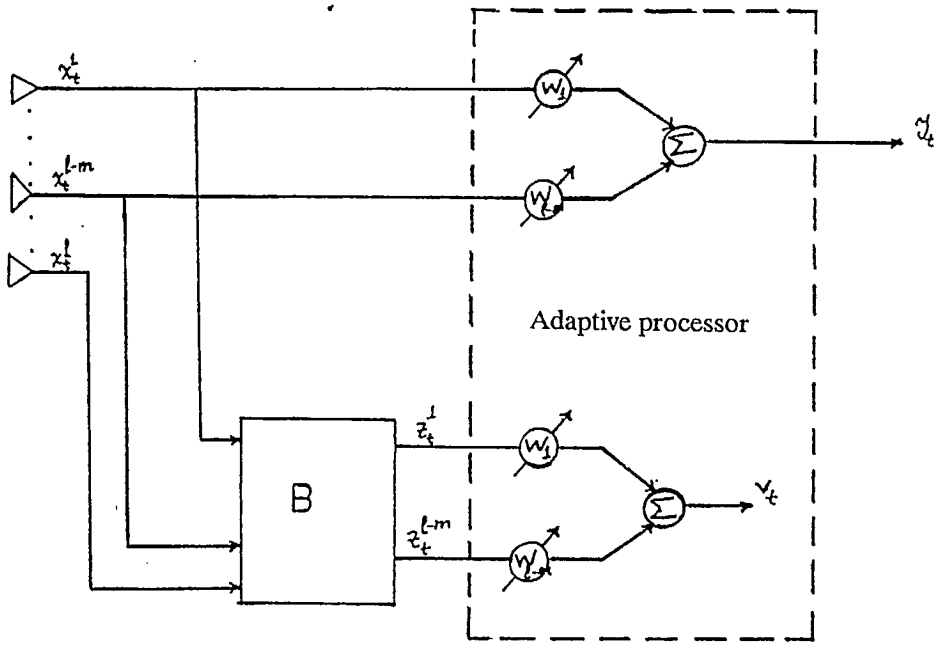

Fig.13 Block diagram for SJNR nulling

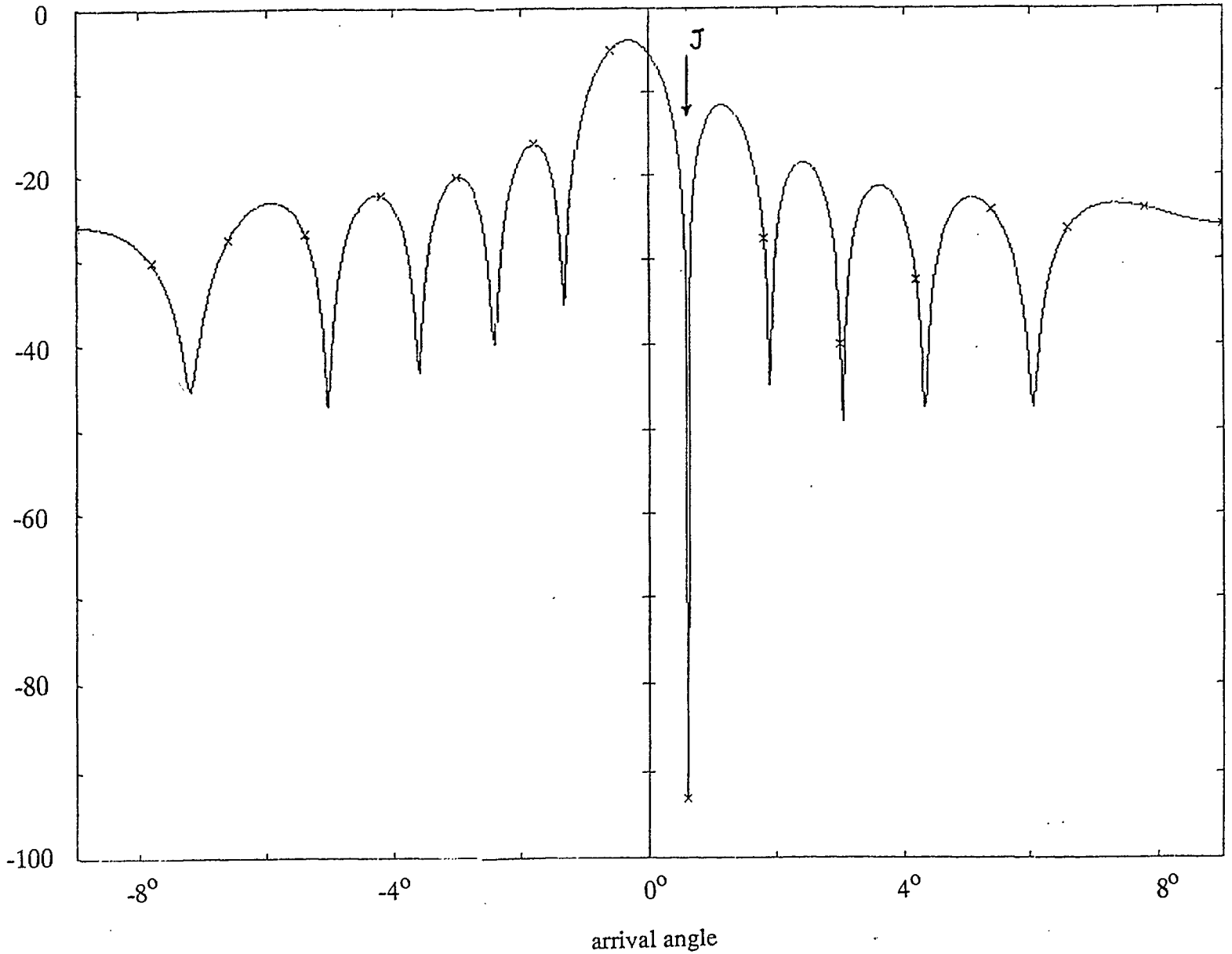

Fig.14 The array pattern after 100 iterations
(L=12, d= $\lambda/2$, $\theta_d = 0^\circ$, $\theta_j = 6^\circ$, SNR=40 db, JNR=70 db)

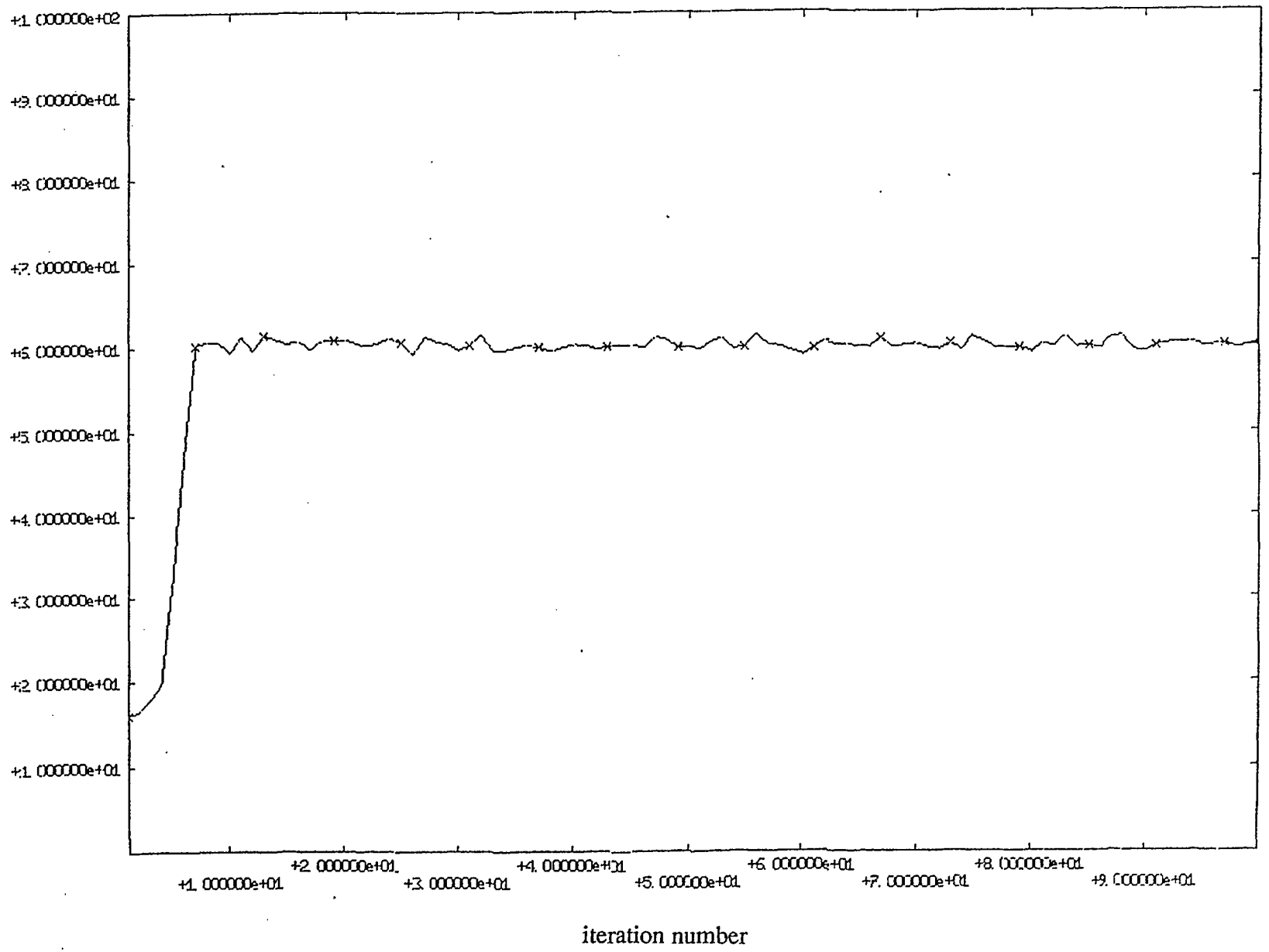

Fig.15 The objective function value versus iteration number, modified conjugate gradient algorithm.

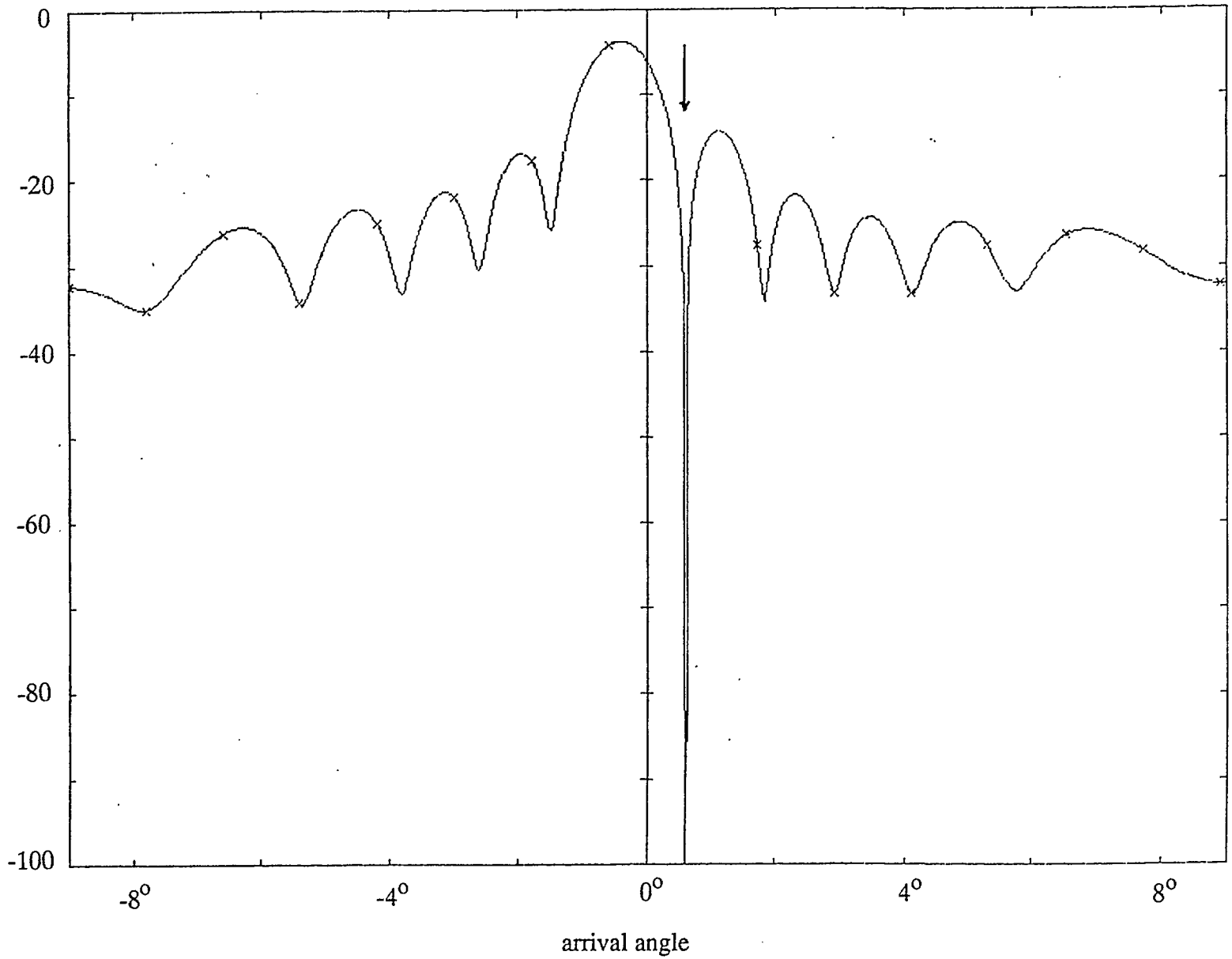

Fig.16 The adapted array pattern using the conjugate gradient after 100 iterations" ($\theta_d = 0^\circ$, $\theta_j = 6^\circ$, $SNR = 40db$, $JNR = 70db$)

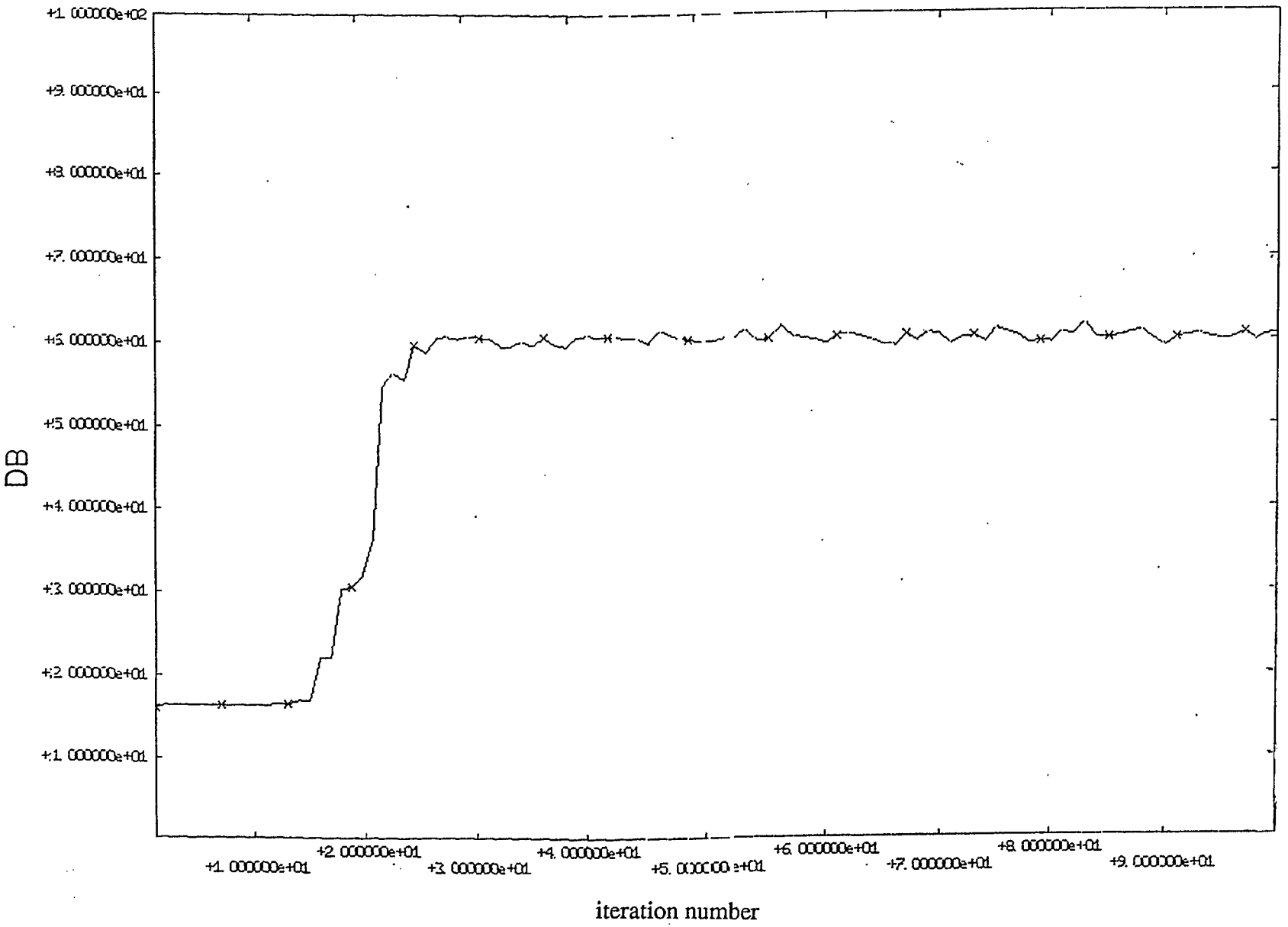

Fig.17 The objective function value versus iteration number, standard conjugate gradient algorithm.

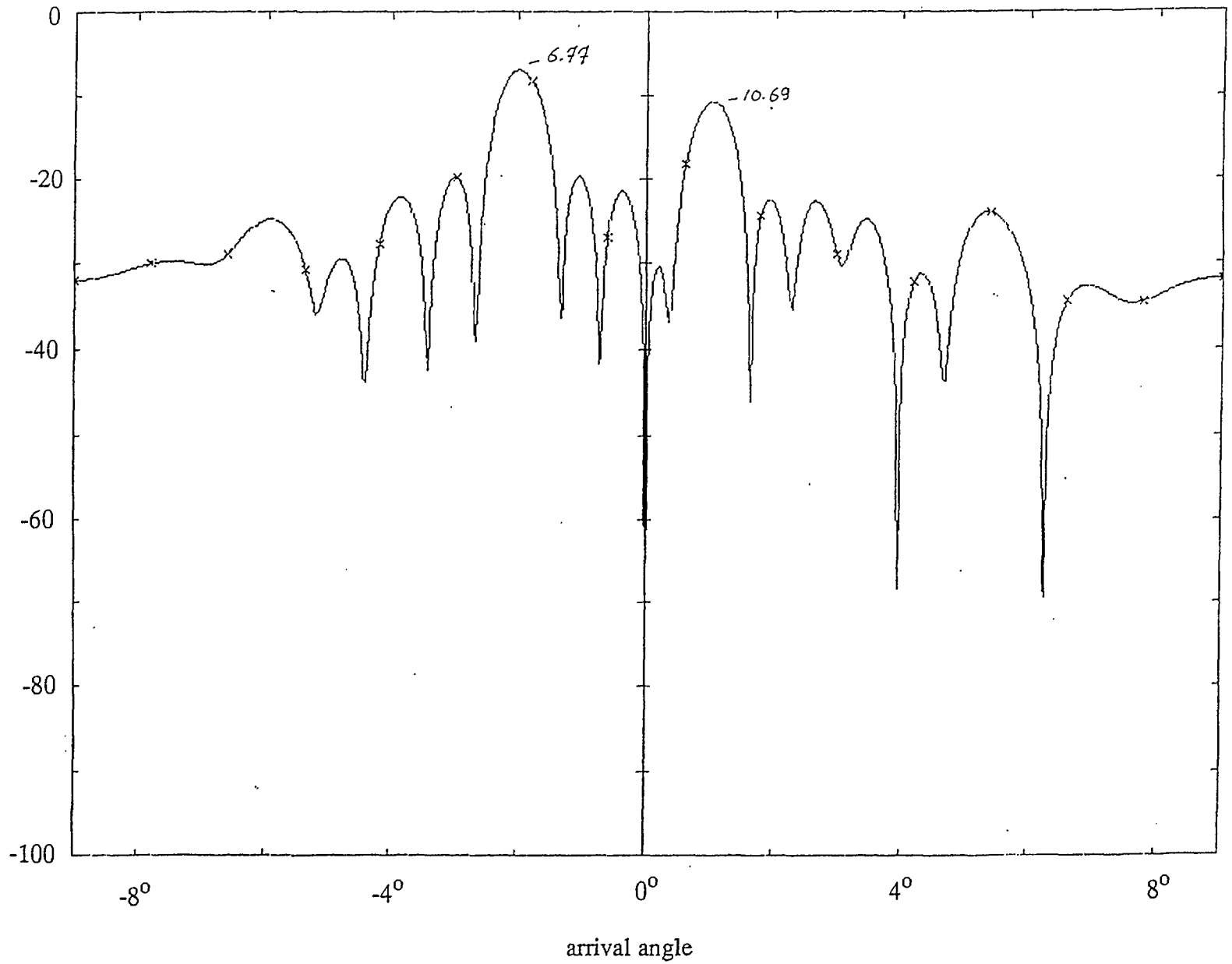

Fig.18 The adapted pattern for two desired signals and single jammer
($\theta_{d_1} = -20^\circ$, $\theta_{d_2} = 10^\circ$, $\theta_j = 0^\circ$) $SNR_1 = 10$ db, $SNR_2 = 0$ db, $JNR = 50$ db

DOCUMENT CONTROL DATA

(Security classification of title, body of abstract and indexing annotation must be entered when the overall document is classified)

1. ORIGINATOR (the name and address of the organization preparing the document. Organizations for whom the document was prepared, e.g. Establishment sponsoring a contractor's report, or tasking agency, are entered in section B.)

UNIVERSITY OF TORONTO

2. SECURITY CLASSIFICATION (overall security classification of the document. including special warning terms if applicable)

UNCLASSIFIED

3. TITLE (the complete document title as indicated on the title page. Its classification should be indicated by the appropriate abbreviation (S,C,R or U) in parentheses after the title.)

Experiments on Dual-Band EHF Controlled-Beam Antennas for Frequency-Hopped Signals: Phase C

4. AUTHORS (Last name, first name, middle initial. If military, show rank, e.g. Doe, Maj. John E.)

J.L. Yen, P. Kremer & N. Amin

5. DATE OF PUBLICATION (month and year of publication of document)

June 20, 1988

6a. NO. OF PAGES (total containing information. Include Annexes, Appendices, etc.)

29

6b. NO. OF REFS (total cited in document)

3

7. DESCRIPTIVE NOTES (the category of the document, e.g. technical report, technical note or memorandum. If appropriate, enter the type of report, e.g. interim, progress, summary, annual or final. Give the inclusive dates when a specific reporting period is covered.)

CONTRACTOR's ANNUAL REPORT

8. SPONSORING ACTIVITY (the name of the department project office or laboratory sponsoring the research and development. Include the address.)

COMMUNICATIONS RESEARCH CENTRE

9a. PROJECT OR GRANT NO. (if appropriate, the applicable research and development project or grant number under which the document was written. Please specify whether project or grant)

32A99

9b. CONTRACT NO. (if appropriate, the applicable number under which the document was written)

DSS No. 36001-6-3562/01-ST

10a. ORIGINATOR'S DOCUMENT NUMBER (the official document number by which the document is identified by the originating activity. This number must be unique to this document.)

NONE

10b. OTHER DOCUMENT NOS. (Any other numbers which may be assigned this document either by the originator or by the sponsor)

NONE

11. DOCUMENT AVAILABILITY (any limitations on further dissemination of the document, other than those imposed by security classification)

( ) Unlimited distribution
( ) Distribution limited to defence departments and defence contractors; further distribution only as approved
( ) Distribution limited to defence departments and Canadian defence contractors; further distribution only as approved
( ) Distribution limited to government departments and agencies; further distribution only as approved
( ) Distribution limited to defence departments; further distribution only as approved
( ) Other (please specify):

12. DOCUMENT ANNOUNCEMENT (any limitation to the bibliographic announcement of this document. This will normally correspond to the Document Availabilty (11). However, where further distribution (beyond the audience specified in 11) is possible, a wider announcement audience may be selected.)

13. ABSTRACT (a brief and factual summary of the document. It may also appear elsewhere in the body of the document itself. It is highly desirable that the abstract of classified documents be unclassified. Each paragraph of the abstract shall begin with an indication of the security classification of the information in the paragraph (unless the document itself is unclassified) represented as (S), (C), (R), or (U). It is not necessary to include here abstracts in both official languages unless the text is bilingual).

Experimental investigation of dual-band IF nulling was performed on a two-beam 43 Ghz adaptive antenna test bench. The static performance of dual-band nulling was compared with that of narrow-band nulling alone. A simple fast algorithm to maximum signal. to jammer and noise ratio is proposed. Simulation results on a simple phase array in nulling performance and convergence speed are presented.

14. KEYWORDS, DESCRIPTORS or IDENTIFIERS (technically meaningful terms or short phrases that characterize a document and could be helpful in cataloguing the document. They should be selected so that no security classification is required. Identifiers, such as equipment model designation, trade name, military project code name, geographic location may also be included. If possible, keywords should be selected from a published thesaurus. e.g. Thesaurus of Engineering and Scientific Terms (TEST) and that thesaurus identified. If it is not possible to select indexing terms which are Unclassified, the classification of each should be indicated as with the title.)

Adaptive antenna, frequency-hopping, anti-jamming ratio, experimental, fast algorithm.